Scanned electrical probe characterization of carrier transport behavior in InAs nanowires

X. Zhou,[b] S. A. Dayeh,[b] D. Aplin, D. Wang, and E. T. Yu[a]
Department of Electrical and Computer Engineering, University of California, San Diego, La Jolla, California 92093-0407 and Materials Science Program, University of California, San Diego, La Jolla, California 92093-0407

(Received 10 February 2006; accepted 10 March 2006; published 25 July 2006)

Conductive atomic force microscopy combined with detailed calculations of electronic subband structure has been used to analyze electron transport behavior across the transition between ballistic and drift/diffusive motion in InAs nanowires grown by metal organic chemical vapor deposition. Using a conducting tip in an atomic force microscope as a local, positionable electrical probe, InAs nanowire resistance as a function of electron transport distance within the nanowire has been measured. For distance of ~200 nm or less, this resistance is observed to be nearly independent of distance, while for larger distances the resistance increases linearly with distance. Analytical calculations indicate that a resistance only weakly dependent on distance should be observed for distances up to a few times the electron mean free path, and calculations of the mean free path using a variety of approaches yield values in the range of ~50 nm, very consistent with the observation of distance-independent resistance for transport distances up to ~200 nm. © *2006 American Vacuum Society.* [DOI: 10.1116/1.2213267]

I. INTRODUCTION

Quasi-one-dimensional systems such as semiconductor nanowires and nanotubes are of outstanding current interest as building blocks for nanoscale electronic and optoelectronic devices.[1–4] However, the detailed nature of carrier transport in such structures remains at present incompletely characterized and understood. For example, the effect of dimensionality on carrier scattering and mobility, the influence of defects and surface electronic structure on carrier transport, and the transition from ballistic transport to motion dominated by drift and diffusion are currently the subjects of active investigation and debate.[5–7] Improved characterization and understanding of these and related phenomena in semiconductor nanowires and related structures will be essential in realizing their full potential for application in electronic, photonic, and other devices and systems.

We have used conductive atomic force microscopy (cAFM) to elucidate the nature of carrier transport in InAs nanowires at the nanoscale. InAs is a particularly intriguing semiconductor material due to its small electron effective mass, correspondingly high bulk electron mobility, and inherent surface accumulation of electrons, and InAs nanowires are currently being explored as candidates for high-performance nanoscale electronic devices.[8–10] For such applications, an understanding of the nature of carrier transport in InAs nanowires, including the possibility and nature of ballistic carrier motion over short distances, is key. Detailed studies of low temperature electron transport in InAs nanowires have been performed,[11] and analysis of electrical characteristics of nanowire field-effect transistor structures has yielded characteristic scattering lengths estimated to be on the order of 100 nm.[12] However, the length scales over which ballistic or nearly ballistic transport can occur in such structures, and the nature of electron transport at distances spanning the transition from ballistic to drift/diffusive motion, remain to be characterized.

To elucidate these issues, scanned probe characterization of electronic structure and transport can provide a powerful complement to macroscopic electrical characterization of nanowire-based devices by offering the ability to perform direct experimental assessment of local electrical behavior with spatial resolution typically in the range of tens of nanometers.[13,14] Using a conducting scanning probe tip as a local electrical contact, we have performed direct measurements of two-terminal resistance as a function of electron transport length within an InAs nanowire. For transport lengths of ~200 nm or less, length-independent resistance indicative of ballistic transport behavior is observed. For greater transport lengths, the resistance is found to increase approximately linearly with length, as expected for conventional drift transport. Calculations performed to estimate the electron mean free path in InAs nanowires based on measured mobilities and model calculations of nanowire electronic structure yield values in the range of ~50 nm, and analysis of expected carrier transport behavior for distances over which only a small number of scattering events is expected confirms that resistance should be only weakly dependent on carrier transport distance.

II. EXPERIMENT

The InAs nanowires employed in these studies were grown by metal organic chemical vapor deposition using colloidal Au nanoparticles ~40 nm in diameter for nucleation on thermally oxidized Si substrates. Growths were conducted at a pressure of 100 Torr and a substrate temperature of

[a]Electronic mail: ety@ece.ucsd.edu
[b]These authors contributed equally to this work.

350 °C, with arsine (AsH_3) and trimethylindium (TMIn) precursors at a V/III flow ratio of 25 for 15 min. A detailed study of the InAs nanowire nucleation and relevant growth mechanisms is discussed elsewhere.[15] The nanowires were unintentionally doped *n* type, and for each growth nanowire diameters typically were in the range of 50–100 nm. Following sonication to release the nanowires into solution, the nanowires were deposited onto a 600 nm SiO_2 layer produced by thermal oxidation on an n^+ Si(001) substrate, on which a patterned and indexed grid structure was previously created. Optical microscopy was used to determine the locations of the randomly positioned nanowires on this grid structure, and then electron beam lithography followed by 15 nm Ti/85 nm Al metallization and a standard lift-off process was used to create Ohmic contacts to the nanowires. The well-known phenomenon of Fermi level pinning above the conduction-band edge of InAs (Ref. 16) enabled ready formation of low-resistance Ohmic contacts to the InAs nanowires.[10]

Scanned probe measurements were performed using a Digital Instruments/Veeco Nanoscope III multimode atomic force microscope to which a current preamplifier was attached to enable cAFM measurements.[17] The experimental geometry employed is shown schematically in Fig. 1(a). A diamond-coated scanning probe tip served as a positionable electrical contact to the InAs nanowire, with the macroscopic Ohmic contact fabricated lithographically serving as the second contact to the nanowire for a two-terminal measurement of electrical current flow through the nanowire. A dc bias voltage V_{sd} was applied between the macroscopic contact and the conducting probe tip and the resulting current was measured as a function of distance *L* between the probe tip and the edge of the contact. The second macroscopic Ohmic contact shown in Fig. 1(a) remained floating, and therefore did not contribute to the current flow observed in these measurements.

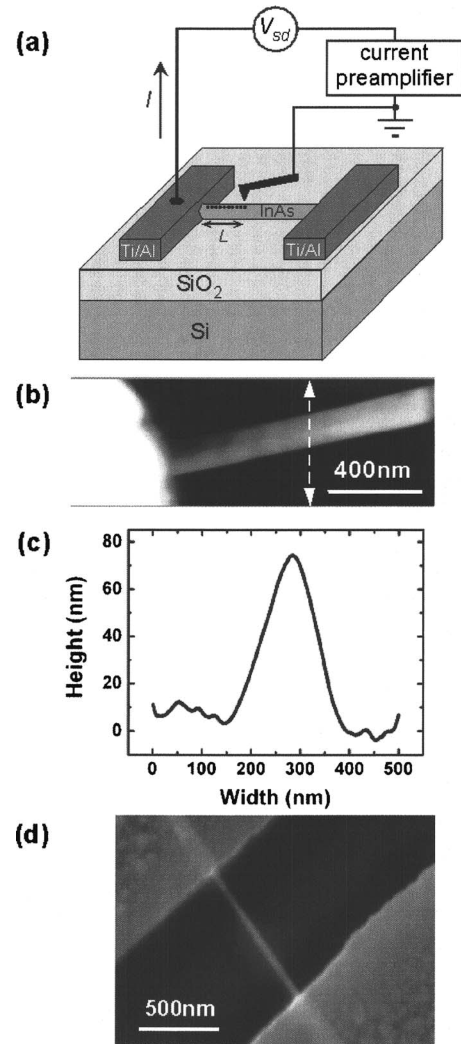

FIG. 1. (a) Schematic diagram of experimental probe tip and sample geometry and electrical measurement configuration. Current *I* is measured for fixed bias voltage V_{sd} as a function of tip-contact distance *L*. (b) AFM topograph of InAs nanowire and Ti/Al Ohmic contacts. (c) Topographic line profile extracted from AFM along the dashed arrow in (b), showing nanowire diameter of ~70 nm as determined from the nanowire height. (d) Scanning electron microscope image showing the InAs nanowire and Ohmic contacts.

III. RESULTS AND DISCUSSION

Figure 1(b) shows an AFM topograph of the InAs nanowire device, consisting of a 75 nm diameter InAs nanowire—determined by the height of the nanowire in the AFM topograph, as shown in Fig. 1(c)—with two Ohmic contacts fabricated as described previously, employed in these studies. A scanning electron microscope image of the nanowire with two Ohmic contacts is shown in Fig. 1(d). Current images acquired at fixed V_{sd} simultaneously with the AFM topograph reveal a trend of constant to decreasing current *I* with increasing tip-contact distance *L*, suggesting that the nanowire resistance contributes significantly to the total device resistance, and as expected generally increases with transport distance within the nanowire. A total device resistance $R \equiv V_{sd}/I$ can then be determined as a function of electron transport distance *L* along the nanowire axis, as shown in Fig. 2. The data in Fig. 2 were derived from cAFM images by averaging current measured at several points across an interval of ~20 nm normal to the nanowire axis and clearly reveal two distinct regimes of behavior. For electron transport distances below approximately 200 nm, *R* is observed to be independent of *L*, while for larger distance *R* increases approximately linearly with *L*. Linear fits to these two regions are also shown in Fig. 2 and yield a constant contribution to the device resistance of ~40 kΩ and, for carrier transport distances over 200 nm, an additional length-dependent contribution of ~23 kΩ/μm.

To interpret these results, we decompose the total measured resistance into several components of distinct physical origin. The total resistance of the tip-nanowire-Ohmic contact structure can be written, adapting the well-known Landauer formalism, as[18]

$$R = R_{\text{drift}} + \frac{h}{2e^2M} + R_{\text{tip-nonowire}} + R_{\text{series}}, \quad (1)$$

where R_{drift} is the contribution due to scattering during drift transport in the nanowire, $h/2e^2M$ is the contact resistance to

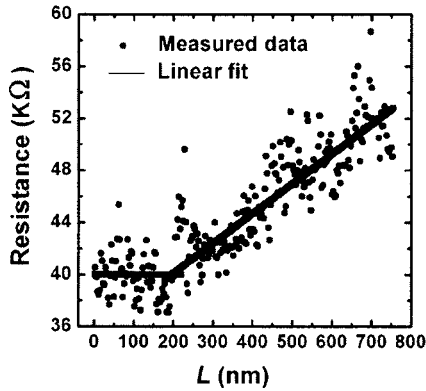

FIG. 2. Resistance measured by cAFM as a function of tip-contact distance L (symbols), with linear fits for L below ~200 nm, for which resistance is independent of L, and for L above ~200 nm, for which resistance increases linearly with L.

the nanowire with M being the number of propagating electron modes in the nanowire, $R_{\text{tip-nanowire}}$ is the additional resistance between the probe tip and the nanowire, and R_{series} is the parasitic series resistance arising from, e.g., external wiring and wire bonds and the patterned metal electrodes. Of these contributions, only R_{drift} depends directly on L; therefore, any dependence observed of R on L should constitute primarily a dependence of the nanowire resistance on L.

The observation of a range of tip-contact distances for which R is nearly independent of L suggests that electron transport over these distances within the nanowire is primarily ballistic. However, the ~200 nm distance over which this behavior is observed should not be taken to be a direct measure of the electron mean free path in the nanowire. Specifically, assuming an electron mean free path Λ, interpreted as the average distance an electron travels in the nanowire before experiencing a scattering event, a nonzero probability t that a single scattering event will result in transmission of the electron (and, consequently, a probability $1-t$ that the electron will be reflected), and a Poisson distribution for the number of scattering events experienced by an electron while traversing a distance L, relatively straightforward calculations show that the resistance of the nanowire increases much more slowly with L, for values up to a few mean free paths, than would be predicted by the conventional scattering-induced resistance,[18]

$$R \approx \frac{h}{2e^2 M}\left(\frac{L}{\Lambda}\right). \tag{2}$$

Thus, the experimental observation shown in Fig. 2 suggests a mean free path approximately in the range of 40–80 nm.

The electron mean free path in the InAs nanowire can also be estimated using independently measured values for electron mobility and calculations of electronic structure within the wire to determine the Fermi velocity. Specifically, the mean free path is given by

$$\Lambda \approx v_F \tau, \tag{3}$$

where ν_F is the Fermi velocity and τ is the scattering relaxation time. τ can be estimated from the electron drift mobility μ using the relation $\mu = q\tau/m^*$, where q is the fundamental electronic charge and m^* is the electron effective mass in InAs. Separate measurements, reported elsewhere, on very similar InAs nanowires have yielded mobility values in the range of 1600–6600 $\text{cm}^2/\text{V s}$.[10] For our purposes we assume an electron mobility for the InAs nanowire of 3000 $\text{cm}^2/\text{V s}$, which combined with the InAs electron effective mass $m^* = 0.023 m_e$ yields a scattering relaxation time $\tau \approx 0.04$ ps. While the measured values of electron mobility in InAs nanowires are much lower than those for bulk InAs, the large contribution of electrons in the InAs surface accumulation layer to carrier transport in the nanowire geometry should lead to effective mobility values closer to the measured mobilities[19,20] of surface electrons in InAs, approximately 1000–3000 $\text{cm}^2/\text{V s}$—as is indeed observed.

To estimate the Fermi velocity, we perform an analytical calculation of the conduction subband structure assuming a model InAs nanowire of radius r with a constant potential $V(r)=0$ within the nanowire and infinite potential barriers $V(r)=\infty$ at the nanowire surface. For this model nanowire structure, Schrödinger's equation in cylindrical coordinates (r,ϕ,z) is separable; the electron wave function can be written in the form $\Psi(r,\phi,z)=\psi(r,\phi)e^{ikz}$ and Schrödinger's equation becomes

$$-\frac{\hbar^2}{2m^*}\frac{\partial^2}{\partial z^2}e^{ik_z z} = E_z e^{ik_z z} \Rightarrow E_z = \frac{\hbar^2 k_z^2}{2m^*}, \tag{4a}$$

$$-\frac{\hbar^2}{2m^*}\left[\frac{\partial^2}{\partial r^2} + \frac{1}{r}\frac{\partial}{\partial r} + \frac{1}{r^2}\frac{\partial^2}{\partial \phi^2}\right]\psi(r,\phi) + V(r)\psi(r,\phi) = E\psi(r,\phi), \tag{4b}$$

where k_z is the wave vector and E_z the corresponding energy for unrestricted motion in the z direction, and E is the quantization energy for bound motion in the (r,ϕ) plane. Equation (4b) is well known and can be simplified to the form[21]

$$\left[\frac{\partial^2}{\partial r^2} + \frac{1}{r}\frac{\partial}{\partial r} + \left(k^2 - \frac{m^2}{r^2}\right)\right]R(r) = 0, \tag{5}$$

where $k^2 = (2m^*/\hbar^2)E$ and $\psi(r,\phi) = R(r)e^{\pm im\phi}$. The solution to Eq. (5) is of the form $\psi(r) = CJ_m(kr)$, where C is a constant and J_m are Bessel functions of the first kind.[15] Assuming a nanowire radius r_0, the eigenvalues of Eq. (4b), which correspond to the discrete conduction subband energies within the nanowire, are given by

$$E_{m,n} = \frac{\hbar^2}{2m^* r_0^2}\rho_{m,n}^2, \tag{6}$$

where $\rho_{m,n}$ is the nth root of the mth order Bessel function J_m. Figure 3 shows the distribution of the first N of these states in energy and the corresponding wave functions.

Using the subband energies given by Eq. (6) and the well-known form of the density of electronic states in one dimen-

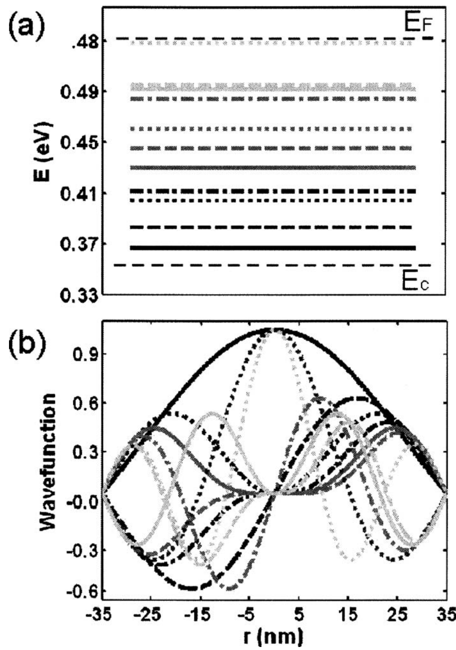

FIG. 3. (a) Calculated conduction subband energies in an InAs nanowire of radius of 35 nm. $E=0$ corresponds to the InAs valence-band edge. (b) Radial wave functions for the subbands shown in (a).

sion, we can then calculate the expected one-dimensional electron concentration n_{1D} as a function of the Fermi energy E_F using the expression

$$n_{1D} = \int_{E_e}^{\infty} D_1(E) f(E) dE \approx \frac{1}{\pi}\left(\frac{2m^*}{\hbar^2}\right)^{1/2} \sum_{E_{m,n}<E_F} \int_{E_{m,n}}^{\infty} \frac{1}{\sqrt{E-E_{m,n}}} \frac{1}{1+e^{(E-E_F)/k_BT}} dE, \quad (7)$$

where $D_1(E)$ is the one-dimensional electronic density of states, E_c is the conduction-band-edge energy, $f(E)$ is the Fermi distribution function, and k_B is Boltzmann's constant. Figure 4 shows n_{1D} calculated from Eq. (7) as a function of the Fermi level position $E_F - E_c$. n_{1D} can be determined experimentally from the 23 kΩ/μm slope of the resistance as a function of carrier transport distance for drift-dominated transport combined with the mobility value cited above and is found by this method to be 9.1×10^6 cm^{-1}.

From Eq. (7) and this experimental value for n_{1D}, we can then determine $E_F - E_c$ and consequently the Fermi velocity v_F and mean free path Λ. Using this approach, we obtain a value for Λ of $\sim$55 nm for an InAs nanowire of radius 35 nm, well within the range of values that are consistent with the observations shown in Fig. 2. As a further check, we can compute the mean free path from Eq. (2), obtaining the number of occupied transverse modes M from the numerical calculation of $E_F - E_c$ and of the conduction subband energies $E_{m,n}$. This approach yields $M=11$ and, using the measured

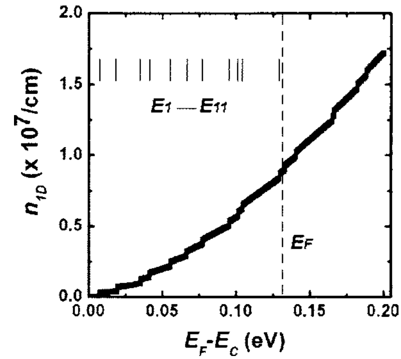

FIG. 4. One-dimensional electron concentration in an InAs nanowire of radius of 35 nm, calculated as a function of Fermi level position.

value for ρ/L of 23 kΩ/μm, a mean free path $\Lambda=51$ nm—very consistent with the first approach and with our experimental observations.

IV. CONCLUSIONS

We have used conductive atomic force microscopy to characterize carrier transport at the nanoscale in InAs semiconductor nanowires, fabricated by metal organic chemical vapor deposition, as a function of electron transport distances spanning the transition from ballistic to drift/diffusive carrier motion. For electron transport distances L within the nanowire of $\sim$200 nm or less, the nanowire resistance is observed to be nearly independent of L, while for larger transport distances the resistance increases approximately linearly with L. These observations suggest that for transport distances of $\sim$200 nm or less, transport is ballistic or nearly ballistic, while for larger distances scattering-induced resistivity eventually dominates and the resistance increases linearly with distance. Model calculations of carrier transmission and total resistance in the nearly ballistic regime, for which the number of scattering events is small and assumed to obey a Poisson distribution, confirm that for distances up to a few mean free paths the resistance should increase much more slowly with L than in the drift transport regime. Calculations of electronic subband structure within the InAs nanowire combined with experimentally determined mobilities, resistance, and carrier concentrations yield, for a variety of approaches, a mean free path of $\sim$50–55 nm, which is very consistent with our experimental observations of resistance as a function of transport distance and analysis of transport in the near-ballistic regime. These results provide important information, critical for high-performance electronic device applications, concerning electron scattering lengths within InAs nanowires and the nature of electron transport over distances near the transition between the ballistic and drift/diffusive regimes of carrier motion.

ACKNOWLEDGMENTS

Part of this work was supported by the National Science Foundation (DMR 0405851 and ECS 0506902) and Office of Naval Research (ONR N000140510149).

[1]Y. Cui, Z. Zhong, D. Wang, W. U. Wang, and C. M. Lieber, Nano Lett. **3**, 149 (2003).
[2]D. D. D. Ma, C. S. Lee, F. C. K. Au, S. Y. Tong, and S. T. Lee, Science **299**, 1874 (2003).
[3]L. Samuelson, *et al.* Physica E (Amsterdam) **21**, 560 (2004).
[4]A. Bachtold, P. Hadley, T. Nakanishi, and C. Dekker, Science **294**, 1317 (2001).
[5]R. Kotlyar, B. Obradovic, P. Matagne, M. Stettler, and M. D. Giles, Appl. Phys. Lett. **84**, 5270 (2004).
[6]K. K. Lew *et al.*, Appl. Phys. Lett. **85**, 3101 (2004).
[7]K. K. Das and A. Mizel, J. Phys.: Condens. Matter **17**, 6675 (2005).
[8]Y. Doh, J. A. van Dam, A. L. Roest, E. P. A. M. Bakkers, L. P. Kouwenhoven, and S. D. Franceschi, Science **309**, 272 (2005).
[9]C. Thelander, T. Martensson, M. T. Bjork, B. J. Ohlsson, M. W. Larsson, L. R. Wallenberg, and L. Samuelson, Appl. Phys. Lett. **83**, 2052 (2003).
[10]S. Dayeh, D. Aplin, X. Zhou, P. K. L. Yu, E. T. Yu, and D. Wang, Nano Lett. (submitted).
[11]C. Fasth, A. Fuhrer, M. T. Björk, and L. Samuelson, Nano Lett. **5**, 1487 (2005).
[12]C. Thelandar, M. T. Björk, M. W. Larsson, A. E. Hansen, L. R. Wallenberg, and L. Samuelson, Solid State Commun. **131**, 573 (2004).
[13]Y. Yaish, J. Y. Park, S. Rosenblatt, V. Sazonova, M. Brink, and P. L. McEuen, Phys. Rev. Lett. **92**, 046401 (2004).
[14]X. Zhou, E. T. Yu, D. Florescu, J. C. Ramer, D. S. Lee, and E. A. Armour, Appl. Phys. Lett. **85**, 407 (2004).
[15]S. Dayeh, D. Aplin, E. Yu, P. Yu, and D. Wang, J. Phys. Chem. B (submitted).
[16]C. A. Mead and W. G. Spitzer, Phys. Rev. Lett. **10**, 471 (1963).
[17]E. J. Miller, D. M. Schaadt, E. T. Yu, C. Poblenz, C. Elsass, and J. S. Speck, J. Appl. Phys. **91**, 9821 (2002).
[18]S. Datta, *Electronic Transport in Mesoscopic Systems* (Cambridge University Press, Cambridge, 1995).
[19]E. Yamaguchi and M. Minakata, Appl. Phys. Lett. **43**, 965 (1983).
[20]Y. Tsuji, T. Mochizuki, and T. Okamato, Appl. Phys. Lett. **87**, 062103 (2005).
[21]P. M. Morse and H. Feshbach, *Methods of Theoretical Physics* (McGraw-Hill, New York, 1953).